Investigation of equilibrium and dynamic performance of $SrCl_2$-expanded graphite composite in chemisorption refrigeration system

Ye Yuan, Huashan Bao*, Zhiwei Ma, Yiji Lu, Anthony P. Roskilly

Sir Joseph Swan Centre for Energy Research, Newcastle University, Newcastle upon Tyne, NE1 7RU, UK

Abstract

This work experimentally investigated adsorption equilibrium and reaction kinetics of ammonia adsorption/desorption on the composite of strontium chloride ($SrCl_2$) impregnated into expanded graphite, and also discussed the potential influence of the addition of expanded graphite on the $SrCl_2$-NH_3 reaction characteristics. The measured and analyzed results can be very useful information to design the system and operating conditions using the similar chemisorption composites. Equilibrium concentration characteristics of ammonia within the studied composite were measured using the heat sources at 90°C, 100 °C and 110°C for the decomposition process, where the degree of conversion achieved 50%, 78% and 96% respectively. Therefore, the equilibrium equation reflecting the relationship between temperature, pressure and concentration was developed, and a pseudo-equilibrium zone was found, which should be useful information to setup the system operating condition for the desired global transformation. It was suspected that the addition of expanded graphite altered the reaction equilibrium due to the pore effect and the salt-confinement. The concept of two-stage kinetic model was proposed and kinetic parameters were determined by fitting experimental data. The developed kinetic equations can predict dynamic cyclic performance of a reactive bed in similar geometric structure with reasonable accuracy. Such a chemisorption cycle using the $SrCl_2$-expnaded graphite (mass ratio 2:1) composite can be used for cooling application, and the maximum SCP value can be achieved as high as 656 W/kg at t=2.5 min, and the COP can be 0.3 after one hour of synthesis process under

* Corresponding author. Tel.: +44 001912084849; Fax: +44 001912226920;
E-mail address: huashan.bao@newcastle.ac.uk

22 the condition of T_{ev}=0°C, T_{con}=20°C,T_{heat}=110 °C.

23 **Keywords:** chemisorption, $SrCl_2$, equilibrium, reaction kinetics, ammonia, refrigeration

Nomenclature

A_c	cross-section area [m^2]
k	rate constant [s^{-1}]
ΔH_{de}	desorption heat [J/mol (NH_3)]
Ar	Arrhenius constant [−]
Ad	constant in kinetic equation [−]
m	parameter in kinetic model [−]
m_d	index constant of kinetics [−]
M	molar mass [kg/mol]
P_c	constraint pressure [Pa]
R	gas constant [J/(mol K)]
t	time [s]
T	temperature [°C]
ΔT	temperature difference [°C]
V	volume [m^3]
x	conversion [−]
Greeks	
v	specific volume [$m^2 \cdot kg^{-1}$]
ρ	density [$kg \cdot m^{-3}$)
Subscripts	

con	condensation
ev	evaporation
d	desorption
eq	equilibrium
a	adsorption
ad	adsorbent
av	average
NH3	ammonia
r	reactor
v	vaporisation

1. Introduction

Chemisorption refrigeration driven by low-grade thermal energy is widely recognised as a promising alternative technology to meet the increasing demand without exacerbating energy and environment pressure. Chemisorption technology has the appealing advantages of wide operating temperature range with numerous reactive materials, simple configuration free of moving parts, liquid pump and separator, higher energy density, and great potential of various applications [1-3]. Metallic halide salt and ammonia is the most commonly used working pair [4].

The chemisorption of $SrCl_2$ ammine/ammonia is one of the potential thermochemical cycles to utilize low grade heat below 100 °C. It has relatively high special adsorption capacity than other ammines/ammonia reaction. Erhard et al. [5] tested a solar powered refrigeration machine based on the $SrCl_2$ ammine/ammonia chemisorption phenomena to maintain the temperature inside a cooling compartment below 6 °C, while the

desorption heat was supplied at around 100 °C by the solar collector by means of two horizontally working heat pipes. The overall efficiency of such a unit in a field test was achieved at 0.05~0.08. Goetz et al. [6] developed and tested a chemisorption refrigeration cycle with two reactors containing $MnCl_2$ and $SrCl_2$ ammines to enable the creation of a heat wave in the flow direction of the heat transfer fluid, so that a significant improvement in the COP could be achieved with a high heat transfer unit in comparison with a single cycle effect using one type of salt ammine. Wang et al. [7] studied the adsorption isotherms of four pure salt ammines with ammonia and confirmed that the $CaCl_2$ and $SrCl_2$ ammines had superior specific adsorption capacity to that of $MnCl_2$ and $BaCl_2$ ammines. Wu et al. [8] studied a two-stage chemisorption cycle using $MnCl_2$-$SrCl_2$-NH_3 sorption working pairs for heat transforming application, and demonstrated its feasibility of achieving a temperature lift from 96 °C to 161 °C with the theoretical exergy efficiency of 0.75. Johannessen et al. [9, 10] designed and studied an ammonia storage and delivery system (ASDS/AdAmmine) with two main cartridges containing the sorbent of $SrCl_2$ ammine compound, of which the feasibility and great competitiveness over urea-SCR system has been demonstrated. The designed $SrCl_2$ sorption system has an ammonia storage capacity of around 450 g/L [10], more than twice that of urea-SCR system; furthermore, the $SrCl_2$-AdAmmine with a dosing temperature at 100 °C reduced tailpipe NOx emission by half of that by urea-SCR system dosing from 180 °C. Jiang et al. [11] investigated a sorption system using the $SrCl_2$+expanded graphite+nanoparticles (carbon coated aluminium) composite for the NO_x reduction for a diesel engine, and found the annual requirement of the $SrCl_2$ composite was much lower than that of urea solution, around 80% lower in mass and 45% lower in volume. Moreover, the addition of the carbon coated aluminium was found to speed up the adsorption/desorption. Bao et al. [12] analysed and evaluated adsorption cycle using two different salt ammines (Case 1) or two identical salt ammines (Case 2) to utilise low grade heat from 60 °C to 180 °C for power generation. Compared to other studied salt ammines ($MnCl_2$, $BaCl_2$, NaBr), the $SrCl_2$–$SrCl_2$ resorption power generation cycle had the highest value of energy density, from 22 MJ/m^3 to 53 MJ/m^3 in the studied temperature

range. The $SrCl_2$–$SrCl_2$ resorption power generation cycle not only had relatively higher work output per mass unit of ammonia but also had higher ammonia uptakes per mass unit of metallic salt (0.751 kg/kg).

However, compared to the aforementioned other typical salt ammines, there is much less information and in-depth study on the characteristics of $SrCl_2$-ammonia chemisorption, which hurdles the development of $SrCl_2$-based system from the very first stage of theoretical assessment. A full understanding of thermodynamic equilibrium, isosteric adsorption and chemisorption kinetics are urgently needed to explore maximum potential, design the process and dimension the system. The data of thermodynamic equilibrium of $SrCl_2$-NH_3 reported in work [13] has been used in many theoretical studies, which uses only one set of equilibrium data to describe adsorption and desorption process without the consideration of the potential hysteresis phenomena. The hysteresis in fact commonly exists in chemical reaction related process and is particularly appreciated to identify the appropriate operating conditions, but scarcely reported. Iloeje et al. [14] mentioned a kinetic model, in which the specific reaction rate as a function of temperature equilibrium drop, with corresponding parameters for $SrCl_2$-ammonia chemisorption in their work but without any details; Huang et al. [15] used the generic format of kinetic model [16] to describe the $SrCl_2/NH_3$ chemisorption, and experimented on a cylindrical bulk of reactant with a volume of 1.76 L to determine the kinetic parameters in the local method, in which the resolution of the kinetic equation coupled with heat transfer in discretisation in space and time since the studied reactive bed had a thickness in radial direction of 70 mm.

In this work, experimental investigation on a lab-scale prototype of chemisorption cycle using the composite of $SrCl_2$ ammine impregnated into expanded graphite has been conducted to firstly determine thermodynamic equilibrium properties with different ammonia concentrations and secondly develop its kinetic model by fitting experimental data. In the last part, the performance of a chemisorption refrigeration system using the studied $SrCl_2$ ammine-expanded graphite composite has been evaluated in terms of the coefficient of performance (*COP*) and the special cooling power (*SCP*).

2. Experiment and measurement

$$SrCl_2 \cdot NH_3 + 7NH_3 \leftrightarrow SrCl_2 \cdot 8NH_3 + \Delta H \quad (1)$$

Based on the reversible reaction between $SrCl_2$ ammine and NH_3 as expressed in Eq. (1), the working principle of a chemisorption cycle in a basic configuration (as present in Fig.1(a)) consists of two phases. The adsorbent bed contains solid adsorbent, and the condenser/evaporator is the refrigerant container. In the first phase, low grade heat is used to drive the desorption process in the adsorbent bed as the adsorbent desorbs refrigerant vapour, while the desorbed refrigerant vapour is collected by the condenser and condensed into liquid as the condensation heat is dissipated to a heat sink. Once this first phase finishes, the adsorbent bed and the condenser were disconnected with a closed valve in the middle, meanwhile their temperature decline down to the ambient level. In the second phase, because of the pressure difference between the adsorbent bed and the condenser, once they are connected again, the chemical reaction occurs spontaneously and the condenser becomes an evaporator as the refrigerant extracts heat from the surroundings and evaporates, and subsequently is adsorbed by the adsorbent in the adsorbent bed. The refrigerant evaporation produces the refrigeration effect while the adsorption occurs in the adsorbent bed releases adsorption heat that needs to be efficiently taken away for the sake of smoothly proceeding adsorption.

The solid composite adsorbent comprised of $SrCl_2$ and expanded natural graphite (ENG) at the mass ratio of 2:1 was studied in this work as it was consolidated into a cylindrical bulk with a density of 300kg/m^3, at a diameter of 52.5 mm with a central hole of 12 mm diameter for gas diffusing channel. It has been extensively proven that the addition of ENG as supporting matrix for composite adsorbent can significantly improve the thermal conductivity and permeability [17-19]. Furthermore, both the mass fraction of ENG and the density of the composite bulk have significant influence on the improvement of thermal conductivity and permeability but in different ways, i.e. the thermal conductivity increases with the increasing mass fraction of

105 ENG and increasing density of composite bulk; whereas, permeability decreases with these two increasing
106 parameters [20]. In order to achieve the accurate measurement of the kinetics of the chemisorption studied,
107 the mass ratio between the salt and expanded graphite and the density of the bulk adsorbent was chosen to
108 minimise the influence of heat and mass transfer performance and to reflect the intrinsic kinetics as much as
109 possible.
110 The composite sorbent was prepared in the following steps: (1) thermal treatment of expandable graphite at
111 600 °C for 10 minutes, as recommended by Tian et al.[21] who compared the thermal conductivity of the
112 expanded graphite that was prepared under different expansion conditions (expansion temperature between
113 300 °C and 800 °C; the expansion duration ranges from 3 min to 90 min); (2) mixing the expanded graphite
114 with $SrCl_2$ aqueous solution thoroughly; (3) drying the mixture in an oven at 120°C for 48 hours to remove
115 all moisture, and sieving the mixture every 30 minutes as any lumps was sifted out and mashed to fine
116 powder before being put back with the rest of mixture powder; (4) directly compress the fine powder into the
117 adsorbent bed. In this instance, provided with the fine powder and the direct compression into the adsorbent
118 bed, it is reasonable to consider good contact between the adsorbent and the metallic wall. Lépinasse et al.
119 [17] studied the adsorbent composite that was prepared using the same method as foregoing, and found that
120 the heat exchange coefficient between the metallic walls and the reactants was in all cases higher than 500
121 $W/(m^2 \cdot K)$, which was almost two orders of magnitude higher than the thermal heat conductivity of the
122 adsorbent composite (4~6 W/m/K). Therefore, the contact resistance was treated negligible.
123 A photograph of the studied test bench is shown in Fig. 1(b). It is a typical single effect chemisorption unit that
124 consists of a cylindrical reactor with a volume of 0.7 L, a 1 m high condenser /evaporator with a volume of
125 0.53 L, a heat source (a heater circulates oil for heat exchange) and a heat sink (a cryostat uses glycol water as
126 heat exchange fluid). One RTD temperature sensor (Omega PT100, with the Class A tolerance of
127 ±(0.15+0.002×T) °C) embedded in the consolidated adsorbent close to the gas channel, its measured data

128 represents the T_2 in Figure 2 that shows the physical model of the adsorbent bed. One thermocouple (K-type
129 with a measurement error of ±0.75%) was used to record the temperature of the heat source fluid (oil). This
130 temperature were also considered to represent the T_1 in Figure 2 due to the high heat transfer coefficient
131 between the heat exchange fluid and the metallic wall and the negligible contact resistance between the metallic
132 wall and the solid adsorbent as foregoing explained. The phenomenon of the adsorbent temperature lagging
133 behind the temperature of the heat exchange fluid is evident due to the limited heat transfer of the adsorbent
134 bed. In addition, considering the small thickness of the adsorbent bulk, it is assumed that the linear temperature
135 gradient between the inner radius (r_2=6mm) and the outer radius (r_1=26.25mm). A mass-average algorithm is
136 used to determine the average temperature of the solid adsorbent, as expressed in Eq. (2).

137 $$\mathrm{T_{av,ad}} = \frac{1}{\rho \mathrm{V}} \int_{r_2}^{r_1} \rho \mathrm{T(r)} \times \mathrm{dV} = \frac{1}{\mathrm{V}} \int_{r_2}^{r_1} \mathrm{T(r)} \times 2\pi \mathrm{rhdr} \quad (2)$$

138 where ρ, V, r and h is the density, volume, radius and height of consolidated composite adsorbent, respectively;
139 T(r) is temperature of consolidated composite adsorbent at radius r, between 6mm and 26.25mm.

140 Each container was instrumented with one pressure transducer (0 ~ 50 bar, Omega PX409-500a, with an
141 accuracy of 0.08% BSL), and one differential pressure sensor (Rosemount, with the accuracy of ±0.075%) was
142 mounted at the bottom of the condenser/evaporator and registered the real-time variation of the mass amount
143 of ammonia in the condenser. To ensure the accuracy of differential pressure sensor, a heat rope was used to
144 wrap on a bypass pipe between the condenser/evaporator and the differential pressure sensor to prevent the
145 formation of liquid ammonia, which could significantly influence the measurement accuracy of the differential
146 pressure sensor. However, the frequently on-and-off working pattern of the heat rope caused some slight
147 pressure change in the bypass pipe which also could be registered by the sensitive differential pressure sensor
148 and generated some noises of the pressure readings. A relief valve (up to 30 bar) was located on the test bench
149 for safety concern. The whole test bench was well insulated to minimize heat loss during the experiment. All

the measured data by various sensors was collected by datataker (DT 85) every 5 seconds.

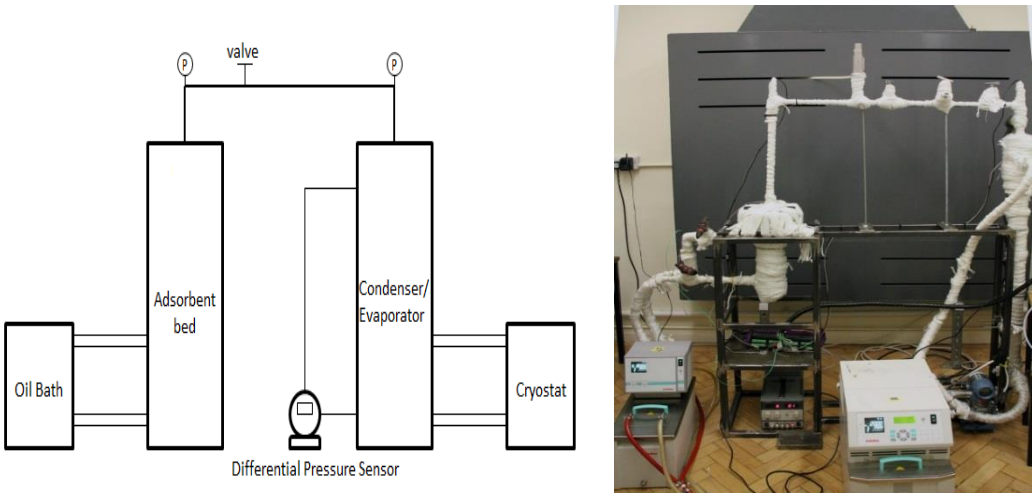

(a) (b)

Figure 1. (a) The schematic and (2) a photo of the chemisorption test bench with heat insulation.

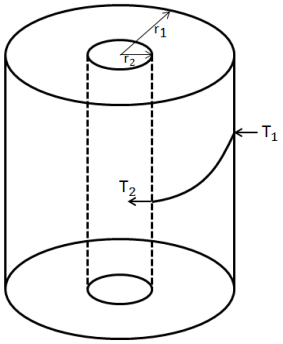

Figure 2. Schematic diagram of physical model.

Unlike the typical measurement of thermodynamic equilibrium that normally performs isochoric processes with step-wise increasing/decreasing temperature, the corresponding equilibrium data is recorded when the measured pressure change become negligible for a reasonably long period of time. This work tested the extreme adsorption/desorption processes with different degree of conversion by carrying out desorption and adsorption separately but individually as thoroughly as possible under three different conditions of heat source temperature (90 °C, 100 °C, 110 °C). Each process proceeds until it reaches equilibrium rather than a continuous complete cycle, and the mass amount of ammonia transferred in each process was calculated according to Eq. (3) [22].

$$\Delta m_{NH3}(\mathrm{t}) = \left(1 - \frac{\upsilon'(T_{ev})}{\upsilon''(T_{ev})}\right) \cdot \frac{\mathrm{A_c}}{\mathrm{g}} \cdot \Delta P_{NH3}(\mathrm{t}) + \frac{V_a}{\upsilon''(T_{ev})} \quad (3)$$

where Δm_{NH3} denotes the mass change of the saturated ammonia in the condenser/evaporator; $\mathrm{A_c}$ is the cross-sectional area of the condenser/evaporator; ΔP_{NH3} is the reading of the differential pressure sensor, representing the pressure difference between two sides of the liquid column; V_{a} is the volume of the condenser/evaporator; $\upsilon'(T_{ev})$ and $\upsilon''(T_{ev})$ is the specific volume of the saturated ammonia liquid and gas respectively. The maximum amount of the transferred ammonia according to the chemical reaction equation Eq.(1) is denoted as $m_{\mathrm{NH3,max}}$ as the stoichiometric ratio between the salt ammine and ammonia is 1:7, then the conversion rate can be calculated as Eq.(4).

$$x(t) = \frac{\Delta m_{NH3}(\mathrm{t})}{m_{NH3,max}} \quad (4)$$

Uncertainty analysis of a multi-variables function $Y = f(\mathrm{n}_1, n_2, \ldots, n_k)$ was carried out using the Eq.(5) [23], hence, the relative error of the average temperature of the composite, $\epsilon_r(\mathrm{T_{av,ad}})$ was $\pm(0.002+0.15/\mathrm{T_{av,ad}})\times 100\%$, and its maximum value was ± 0.88%; the maximum relative error of $\Delta m_{NH3}(\mathrm{t})$ and $x(t)$ was ±0.53%.

$$\epsilon_r(Y) = \sum_{i=1}^{k} \left|\frac{\partial f}{\partial n_i}\right| \frac{\epsilon(n_i)}{Y} \quad (5)$$

The experiment procedure is described as follows, and the experimental results are shown in Table 1.

1. During the desorption testing, the valve was kept closed until the temperature of the circulating oil reached the heat resource temperature (90°C, or 100°C, or 110°C) to supply the adsorbent bed with desorption heat, while the temperature of the condenser was maintained at (20 ±1) ºC by a cryostat as it imitated a coolant source at 20 ºC. The desorption was terminated when the reading of differential pressure sensor was almost unchanged, and then the valves was closed again.

2. During the adsorption testing, the condenser/evaporator was subject to a temperature of (0 ±1) ºC to mimic the environment that needs to be cooled down further, and the valves was kept closed until the temperature of adsorbent bed decreased down to environment temperature. The measurement proceeded until the reading of differential pressure sensor become almost constant.

It normally took up to several hours for each testing, at the end of which the state of reaction can be considered at equilibrium. Experiments on equilibrium with different ammonia concentration was expected to reveal more information related to pseudo-equilibrium area and the hysteresis phenomena, that is significant for the design of system operation to achieve desired performance.

Table 1. Experimental results

Experiment conditions	**90 °C-20 °C-0 °C**		**100 °C-20 °C-0 °C**		**110 °C-20 °C-0 °C**	
Process	de	ad	de	ad	de	ad
T_2, °C	63.1	27.1	69.6	28.2	75.6	31.9
Heat source/Heat sink temperature, °C	90	20.2	100	20.2	110	20.6
$T_{av,ad}$, °C	69.8	21.9	77.2	22.2	84.2	24.9
P_{eq}, Bar	8.5	0.49	8.4	0.46	8.3	0.44
Mass of desorbed ammonia, g	75.2		127.9		148.1	
Concentration (g NH_3/g adsorbent)	0.250		0.110		0.020	
Conversion (x)	50%		78%		96%	

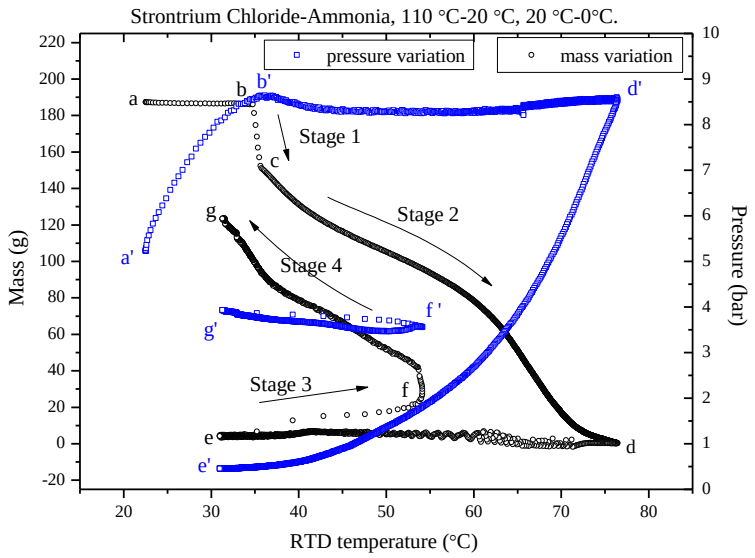

195

196 Figure 3. The variation of the transferable ammonia mass within the adsorbent and the working pressure

197 against the adsorbent bed temperature.

198 **3. Equilibrium calculation and data fitting**

199 Figure 3 shows the variation profile of the mass of adsorbed ammonia and the working pressure against the

200 measured temperature (T_2) during the desorption using the heat source temperature at 110 °C and the

201 corresponding adsorption. The real desorption and adsorption with effective ammonia mass changes seemed

202 to go through two different stages for each as denoted in the figure, and there was a non-mass change phase

203 prior to each process. The whole cycle went like this: (1) initially, both the adsorbent bed and the condenser

204 were kept at heat sink temperature (20 °C). During the phase a-b, the adsorbent bed was heated up from the

205 ambient temperature to the pre-defined temperature (110 °C in this example) and the pressure ascended, while

206 the condenser was maintained at 20 °C. (2) Once the adsorbent bed pressure reached the saturated pressure of

207 the ammonia at 20 °C (around 8.6 bar) in the condenser, the isobaric desorption initiated and the fast reaction

208 occurred, leading to the dramatic drop of the mass of adsorbed ammonia as the Stage 1 shown (phase b-c).

209 Afterwards, the desorption rate gradually slowed down in the Stage 2 (the phase c-d). This is a very common

210 phenomenon for chemical reaction to have such a drastic change at the very beginning of the process. Because

the driving force of the reaction was the pressure difference between the current state and the equilibrium condition, and it was relatively large at the beginning to drive the Stage 1 fast reaction, in return leading to the sharp decrease of this pressure difference (potentially partially attributed to the heat and mass transfer limitation), consequently the reaction rate sharply reduced afterwards in the Stage 2. (3) When the desorption was finished, the adsorbent bed was isolated from the condenser and cooled down to the ambient temperature again as the pressure dropped from point d' to point e' (at a vacuum level). This corresponded to the non-mass change phase before the adsorption. In the meantime, the condenser switched to the evaporator and was cooled down to 0 °C to mimic the environment needs to be cooled down further, and the evaporator pressure was 4.8 bar. (4) Because of the big pressure difference between the adsorbent bed and the evaporator, once they were linked together a fast evaporation and adsorption occurred (as the Stage 3 shown, the phase e-f), at the same time the system pressure jumped to the value of 3.5 bar (a level in the middle of these two pressures). This fast reaction rate caused large quantity of heat release, while the inefficient heat transfer was not able to timely remove the adsorption heat, leading to the considerable increase in the reactor temperature and decrease in equilibrium temperature drop. Subsequently, the reactor temperature dropped as the reaction rate slowed down again in the Stage 4 of the phase f-g.

Chemisorption equilibrium is mono-variant according to the Gibbs phase rule, which means the equilibrium status of system can be identified with the information of either temperature or pressure. However, the $SrCl_2$ ammines-ammonia chemisorption in this work was observed evidently bi-variant with hysteresis. Like the physisorption has typical bi-variant, the equilibrium reflects the relationship between temperature, pressure and ammonia concentration. Similar phenomenon was also found for the $BaCl_2$ ammine/NH_3 chemisorption when the composite of $BaCl_2$/expanded vermiculite were tested [24] and also for the hydration of calcium nitrate when it was tested in a composite bulk mixed with silica gel [25]. The possible explanation is associated with the pore effect and the confinement of the salt inside the pores. Each micro crystallite undergoes a mono-

variant adsorption or desorption following the thermodynamic equilibrium determined by the van't Hoff equation; however, the non-uniform sizes of the pores and micro crystallites may lead to the heterogeneous phase transition across over the whole reactive bulk. Hysteresis may be related to the phenomenon of expansion and contraction of the solid salt-ammonia complex in synthesis and decomposition, respectively. There is an activation barrier for the expansion of solid but never be recovered on contraction, which implies the irreversible energy loss during a complete chemisorption cycle [24,25].

As shown in Table 1, different ammonia concentration were achieved by using different temperature heat sources. To determine each transition line representing the equilibrium with different ammonia concentration, two data points were selected to fit the van't Hoff equation for equilibrium: (1) at the end of each lengthy desorption, the equilibrium in reactor was assumed to achieve at a temperature that was close to heat source temperature, and the measured pressure data at the end of the process represented the equilibrium pressure at this temperature (P_{eq} in desorption in the Table 1). (2) the subsequent adsorption started with the same ammonia concentration with that of the previous desorption, and the onset data of adsorption represented the equilibrium status corresponding to the heat sink temperature (P_{eq} in adsorption in the Table 1), because before the adsorption really occurred the adsorbent reactor was cooled down for a sufficiently long time to make sure the adsorption process start at the heat sink temperature. The developed expression of transition line was shown in Table 2.

Table 2. Transition lines of $SrCl_2$ ammine/NH_3 chemisorption with different ammonia concentration.

Concentration (g (NH3)/g (composite adsorbent))	Transition line	Degree of conversion
0.25	$\ln p_{NH3} = 5.98\frac{-1000}{T} + 31.06$	50% decomposition
0.11	$\ln p_{NH3} = 5.55\frac{-1000}{T} + 29.48$	78% decomposition

0.02	$\ln p_{NH3} = 5.08\frac{-1000}{T} + 27.85$	96% decomposition

252

253 To correlate the transition equilibrium with the value of ammonia concentration, the expression proposed by
254 Zhong et al. [24] as Eq. (4) was used to describe the relationship between temperature, pressure and ammonia
255 concentration of $SrCl_2$-NH_3 chemisorption.

256 $$\mathrm{Ln}P_{\mathrm{NH3}} = (A + B \cdot x)\frac{-1000}{T} + (C + D \cdot x) \quad (4)$$

257 where *x* is the ammonia concentration in the unit of g/g, i.e. the mass amount of adsorbed ammonia inside the
258 composite (salt + expanded graphite). Figure 4 shows the linear fitting of the item of (A+Bx) and (C+Dx) in
259 Eq.(4) for the $SrCl_2$ ammine desorption equilibrium, both of which have the Adjustment R-Square higher than
260 0.95, and the determined parameters are summarised in Table 3. Based on this new correlation, a pseudo
261 equilibrium zone of $SrCl_2$ ammine ad/desorption is plotted in Figure 5, bounded by the lines representing 0%
262 decomposition and 100% decomposition respectively. The single equilibrium line reported in the [13] was also
263 reproduced in Figure 5, which almost overlaps with the 100% decomposition line obtained in this work. That
264 confirms the threshold of thermal conditions for desired decomposition performance, however, because of the
265 existence of pseudo equilibrium zone, this single equilibrium line is not a suitable reference for the precise
266 design of the operating conditions for synthesis process.

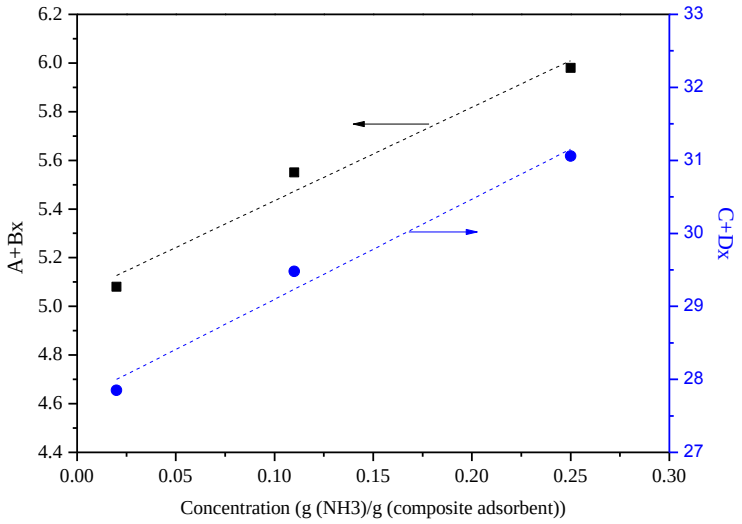

Figure 4. Data fitting of $SrCl_2$ ammine desorption equilibrium based on the Eq. (4).

Table 3. The parameters of equilibrium equation of $SrCl_2$ ammine decomposition.

A	*B*	Adj. R-Square	*C*	*D*	Adj. R-Square
5.050	3.840	0.955	27.725	13.725	0.98

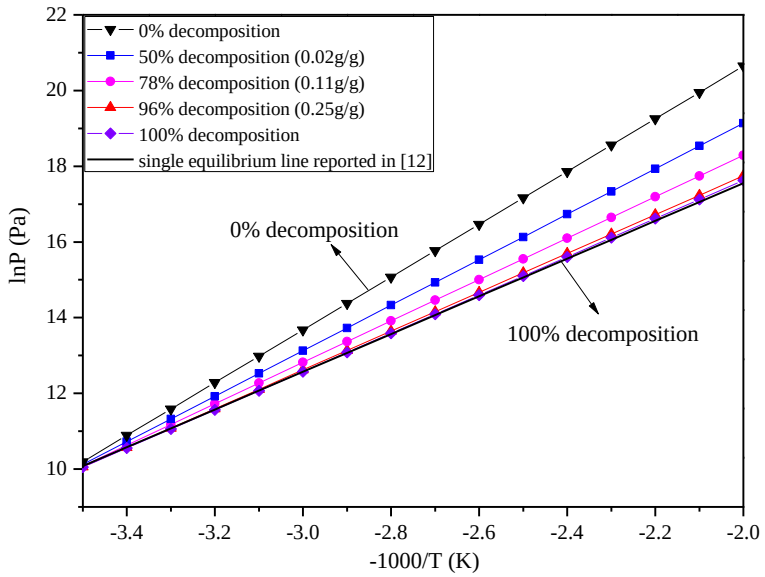

Figure 5. The pseudo-equilibrium zone of $SrCl_2$ ammine desorption on the Clapeyron diagram.

4. Kinetic equations

The general form of the reaction rate is given as Eq. (5) [16].

$$\frac{dx}{dt} = k(P,T)f(x) \tag{5}$$

where x is the degree of conversion of the reaction, i.e. the ratio of mass of actual reacted ammonia and mass of maximum reacted ammonia; the term of k (P, T) is known as specific rate representing the influence of the deviation of operating conditions from equilibrium conditions on the reaction rate for reversible chemisorption. Numerous forms of k (P, T) have been proposed by different researchers. The most commonly used expression of the linear function [16], where the Arrhenius term is considered to practically equivalent to a constant during the reaction, has been used in this work to determine the kinetic parameters of the $SrCl_2/NH_3$ chemisorption in a global model with uniform temperature and pressure throughout the composite adsorbent. Such a method reasonably simplifies the numerical calculation but provide sufficient information for preliminary system plan and system optimal control. The used equations of adsorption and desorption are given as Eq. (6) and (7) [26,27].

Adsorption $$\frac{dx}{dt} = Ar_a \cdot (1-x)^{m_a} \cdot (1-\frac{P_{eq}}{P_c}) \tag{6}$$

Desorption $$\frac{dx}{dt} = Ar_d \cdot x^{m_d} \cdot (1-\frac{P_{eq}}{P_c}) \tag{7}$$

Where Ar and m are constants to be identified; P_{eq} is the equilibrium pressure corresponding to the average temperature of the adsorbent; P_c is the constraining pressure for the reaction, corresponding to the liquid-vapour equilibrium at the temperature of the heat source/sink in the condenser-evaporator. The kinetic parameters determined by fitting the experimental data are shown in Table 4.

The comparison of experimental data and simulation on kinetics of ammonia adsorption/desorption on the $SrCl_2$/expanded graphite composite is displayed in Figure 6. The adsorption kinetic curves show acceptably good agreement between the simulation and experimental data of all cases studied in this work, they were under the same thermal conditions but had different initial concentration of ammonia. However, there is

noticeably discrepance between the simulation and experimental data of desorption kinetics under the desorption conditions of 90 °C-20 °C and 100 °C -20 °C, mainly in the beginning part of the processes. As aforementioned, it seemed to go through two stages at different reaction rates to complete a decomposition, the first stage involved a relatively faster reaction rate while at the second stage it suddenly slowed down a lot and afterwards continuously reduced.

Therefore, to better reflect this phenomenon and the influence of the constraining temperature on the kinetics, an adjustment to the kinetic equation is necessary to more accurately describe the global transformation. The concept of two-stage desorption kinetic model was adopted in this work as given in Eq. (8), and the value of the additional parameters are given in Table 4. Figure 7 shows the good agreement between experimental results and simulation based on the proposed model for decomposition. It is worth noting that this two-stage model is more suitable for the situations when the heat source temperature is not sufficiently high and the heat transfer performance is less competent, and the reactor experiences a large temperature jump at the beginning of desorption as a real adsorption heat pump/refrigeration application normally would experience, temperature jumping from heat sink temperature to heat source temperature as it switches to the next cycle. Otherwise, the kinetic equations in the format of Eq. (6) and (7) using the values of kinetic parameters in Table 4 should reasonably accurately describe the global transformation.

$$\frac{dx}{dt} = (\mathrm{Ar}_d + \mathrm{Ad} * \mathrm{T}) \cdot \mathrm{x}^{m_d} \cdot (1 - \frac{P_{eq}}{P_c}) \quad (8)$$

By using the multi-stage fitting adjustment, the relative error of the simulated global transformation against the measured data was less than 10% for the case of 100°C -20°C and less than 5% for the case of 90°C - 20°C.

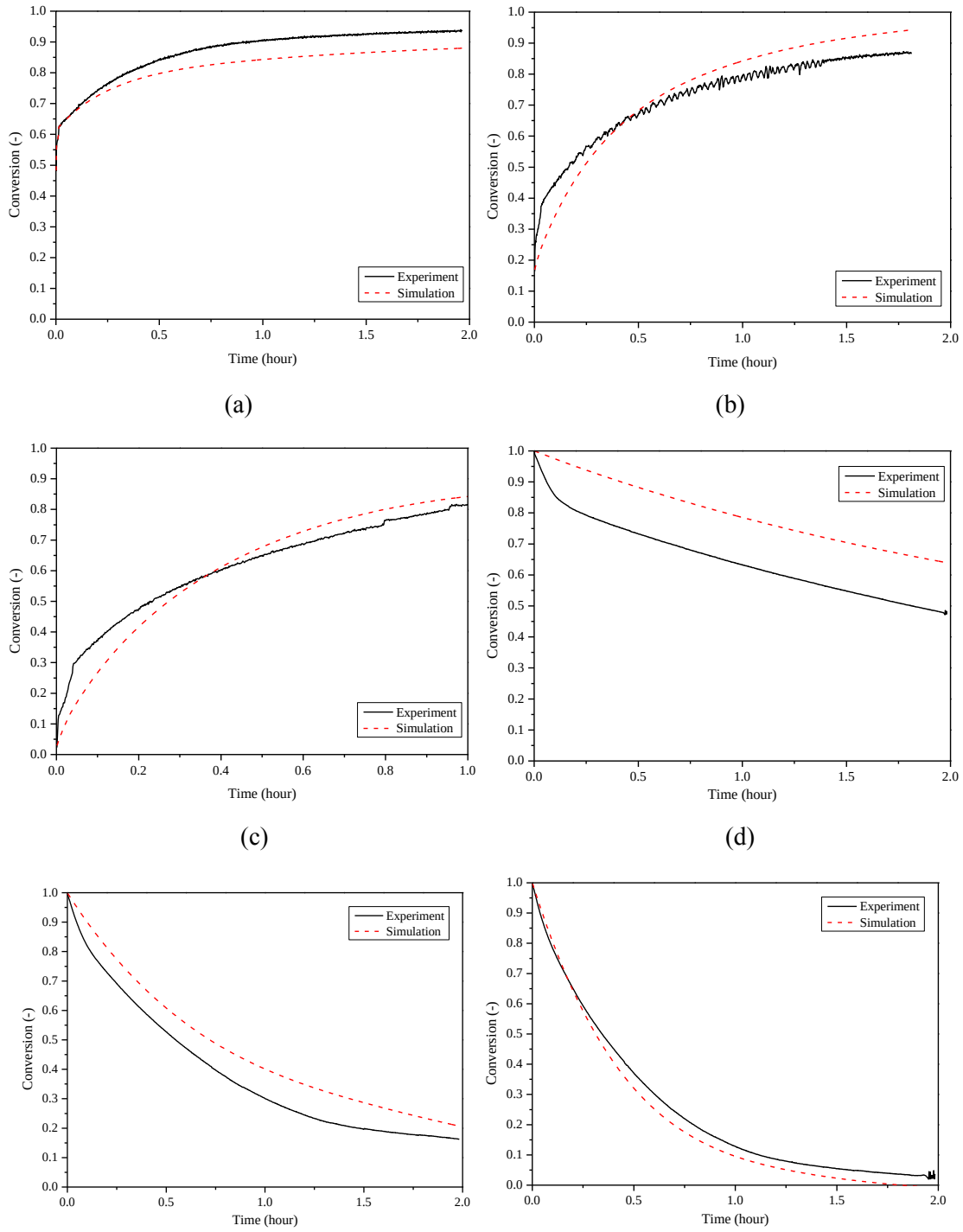

Figure 6. Kinetic curves of ammonia adsorption/desorption on the $SrCl_2$/expanded graphite composite. (a) adsorption (90°C-20°C); (b) adsorption (100°C-20°C); (c) adsorption (110°C-20°C); (d) desorption(90°C-20°C); (e) desorption(100°C-20°C); (f) desorption(110°C-20°C);.

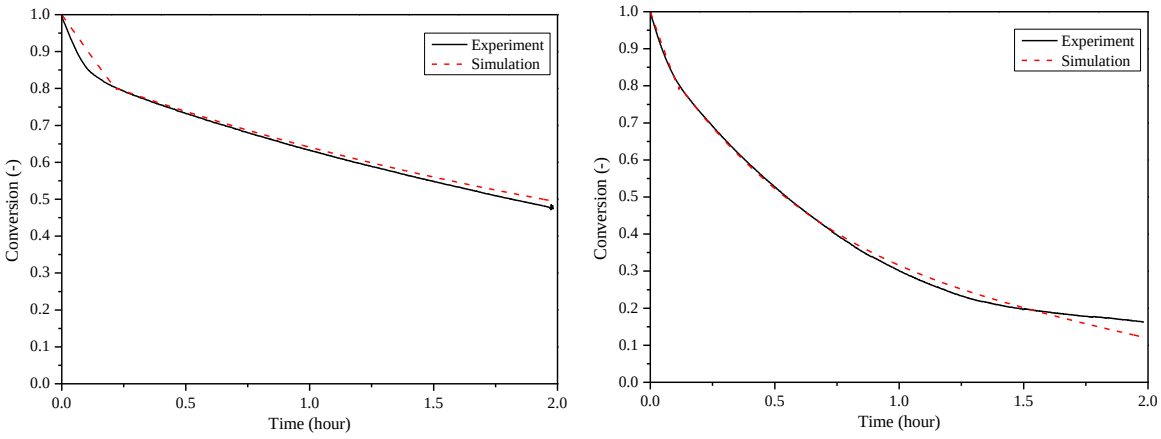

(a) (b)

Figure 7. Comparison between experiment and simulation based on the modified kinetic model of ammonia desorption from the $SrCl_2$/expanded graphite composite. (a) 90°C-20°C; (b)100°C -20°C.

Table 4. The kinetic parameters of the $SrCl_2/NH_3$ chemisorption.

		Ar	*Ad*	*m*
Adsorption		0.001631		2.071
Desorption	Stage 1 (x>0.8)	0.02413	-6.2×10^{-8}	1.1
	Stage 2(x<0.8)	0.0004598		1.1

5. Refrigeration system performance

Based on the experiment data, the *SCP* and *COP* of the tested chemisorption prototype using $SrCl_2$-expanded graphite composite adsorbent was evaluated using Eq.(11) and Eq.(12) for the refrigeration at 0 °C when three different heat source temperature were used (90 °C, 100 °C, 110 °C) while the heat sink temperature was at 20°C.

$$Q_{\mathrm{cool}}(\mathrm{t}) = \Delta m_{\mathrm{NH3}}(\mathrm{t}) \cdot \Delta H_{\mathrm{NH3,v}} - (m_{\mathrm{NH3}} \cdot C_{\mathrm{p,NH3}} + m_{\mathrm{e}} \cdot C_{\mathrm{p,e}}) \cdot (T_{\mathrm{con}} - T_{\mathrm{ev}}(t)) \quad (9)$$

$$Q_{\mathrm{heat}} = (m_{\mathrm{ad}} \cdot C_{\mathrm{p,ad}} + m_{\mathrm{r}} \cdot C_{\mathrm{p,r}}) \cdot (T_{\mathrm{d}} - T_{\mathrm{a}}) + \Delta m_{\mathrm{NH3}}(\mathrm{t}) \cdot \Delta H_{d} \quad (10)$$

$$SCP(\mathrm{t}) = \frac{Q_{\mathrm{cool}}(t)}{m_{\mathrm{ad}} \cdot \Delta t} \tag{11}$$

$$COP\ (\mathrm{t}) = \frac{Q_{\mathrm{cool}}(t)}{Q_{\mathrm{heat}}} \tag{12}$$

where $\Delta H_{\mathrm{NH3,v}}$ is the vaporization heat of the ammonia; m_{NH3} is the total mass of ammonia in the condenser/evaporator; m_{e} is the metal mass of the evaporator; m_{ad} is the total mass of the composite adsorbent; m_{r} is the mass of the metallic reactor; t is the time point in the synthesis process, and Δt is the duration of the whole synthesis process; ΔH_d is the desorption heat that can be calculated from the equilibrium lines shown in Table 2. As described before, the decomposition undertook for a long time to ensure the completeness of the reaction so that the function of the heat input Q_{heat} in Eq.(10) is independent of time; whereas, the focus is on the synthesis process with cooling output Q_{cool}, the instantaneous variation of which is calculated as given in Eq.(9) for the evaluation of SCP and COP value. In fact, the actual Q_{heat} in the present experiment was originally supplied by the heater in the thermal oil bath, which should be higher than the calculated value based on Eq.(10) due to considerable heat loss through poor insulation of the thermal bath and the pipeline of the circulating hot oil and heat transfer losses. However, the performance evaluation based on the Eq. (9-12) represent a more generic evaluation of the potential cycle COP and SCP without taking into account of the negative impact of the imperfect design of adsorbent bed and other system components on the overall performance. It was aimed to explore the maximum potential of the cycle performance using the studied composite, which is very important information for the system design and optimization and a fair comparison with other different technologies.

Figure 8 shows the varying value of the *SCP* and *COP* of the studied system with respect to the process duration under different conditions. As expected, the *SCP* value reaches its summit at the very beginning of the process due to the fast reaction (at the Stage 1 of desorption). With the highest degree of conversion in the desorption using 110 °C heat source, the maximum *SCP* achieved was 656 W/kg at around t = 2.5min, while the *COP*

value at the same time was only around 0.07; as the reaction went on, the *SCP* value drastically dropped, on the contrary the *COP* value gradually ascended along the ongoing process and eventually reached the highest value of 0.3 at the end of the one-hour synthesis when the achieved conversion was only 58% of that in desorption. The COP value could achieve 0.5 if it reached 100% conversion as the desorption has achieved, nevertheless, in this instance, much longer cycle time is required and the *SCP* value would be unfavorable.

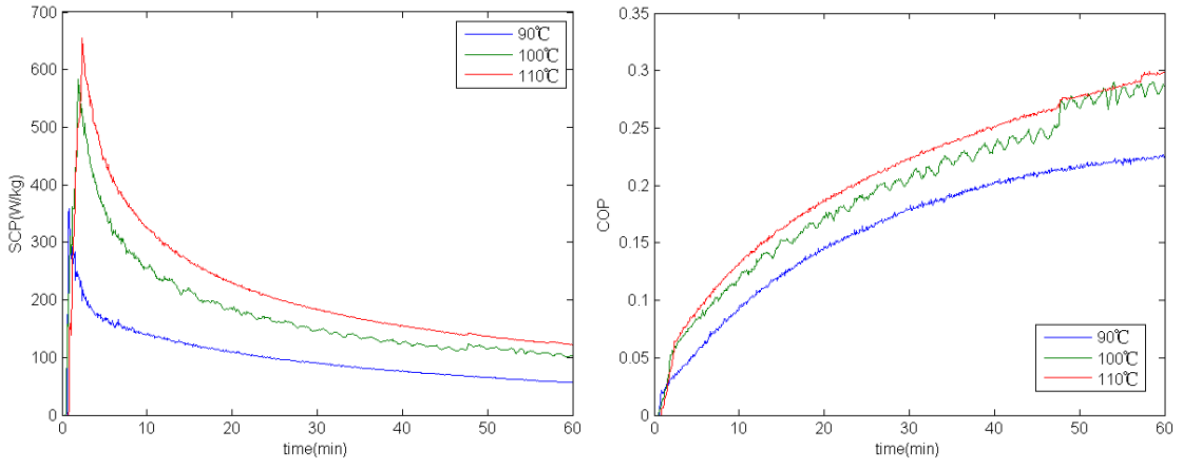

(a) (b)

Figure 8. The performance of the $SrCl_2$-NH_3 chemisorption system for refrigeration at 0 °C when heat sink temperature at 20 °C with different heat source temperature. (a) *SCP*; (b) *COP*.

6. Conclusion

The isotherms and dynamic ad/desorption performance of the ammonia chemisorption using the composite of $SrCl_2$ ammine and expanded graphite at the mass ratio of 2:1 was experimentally investigated using different heat source temperatures (90 °C, 100 °C, and 110 °C) and heat sink temperature at 20 °C for cooling application at 0 °C. Because of the limited heat transfer property of the reactor, the actual adsorbent temperature was about 20~30 °C lower than the heat exchange fluid temperature. The desorption using 90 °C heat source (the maximum composite temperature only at 70 °C) only achieve 50% of conversion despite of lengthy duration; while 100% conversion could be realized by using 110 °C heat source (the maximum composite temperature only at 84.2 °C). The phase transition of the studied chemisorption composite was found bi-variant equilibrium,

which was defined by the relationship between temperature, pressure and ammonia concentration. A pseudo equilibrium area existed and was encompassed by the 0% desorption equilibrium and 100% desorption equilibrium lines. Considering the theoretical mono-variant equilibrium of pure salt, the possible reason of the bi-variant equilibrium of the composite was speculated to be associated with the pore effect, the confinement of the salt inside the pores. If the mass fraction of expanded graphite as the porous matrix in the composite is changed, the bi-variant equilibrium correlation may need to be re-measured, which will need further confirmation.

The concept of two-stage desorption kinetic model was proposed and adopted to better reflect the experimental phenomenon and the influence of the constraining temperature on the kinetics. Based on the experimental data, the kinetic parameters of the ammonia ad/desorption on the studied composite were determined and the developed kinetic equations can predict the global transformation with reasonable accuracy. This two-stage model is more suitable for the cases when the reactor experiences a large temperature jump at the beginning of desorption, i.e. jumping from heat sink temperature to heat source temperature, and the heat transfer performance is relatively inefficient.

A basic chemisorption cycle using the studied $SrCl_2$-expanded graphite composite was evaluated in terms of system *SCP* and *COP* for the cooling application (T_{ev} = 0 °C, T_{con}=20 °C). The maximum *SCP* value is potentially obtained as 656 W/kg when using 110°C heat resource; while the highest *COP* value as 0.3, appears at the end of the process.

Acknowledgement

The authors gratefully acknowledge the support from the Heat-STRESS project (EP/N02155X/1) and Centre for Energy Systems Integration (EP/P001173/1) funded by the Engineering and Physical Science Research

Council of the UK.

Reference

[1] Wang RZ, Wang LW, Wu JY. Adsorption refrigeration technology: Theory and application. Wiley 2014.

[2] R.Z. Wang, Z.Y. Xu, Q.W. Pan, S. Du, Z.Z. Xia. Solar driven air conditioning and refrigeration systems corresponding to various heating source temperature. Applied Energy, 169, 2016, 846-856.

[3] H.S. Bao, Z.W. Ma, A.P. Roskilly. Integrated chemisorption cycles for ultra-low grade heat recovery and thermos-electric energy storage and exploitation. Applied Energy, 164, 2016, 228-236.

[4] H S Bao, R Z Wang. A review of reactant salts for resorption refrigeration systems. International Journal of Air-Conditioning and refrigeration. 165, 2010.

[5] A. Erhard, K. Spindler and E. Hahne. Test and simulation of a solar powered solid sorption cooling machine. International Journal of Refrigeration. 21(1998) 133-141.

[6] V. Goetz, J. Llobet. Testing and modelling of a temperature front solid-gas reactor applied to thermochemical transformer. Applied Thermal Engineering, 20(2000)155-177.

[7] L. Wang, L.Chen, H.L.Wang, D.L.Liao. The adsorption refrigeration characteristics of alkaline-earth metal chlorides and its composite adsorbents. Renewable Energy, 34(2009) 1016-1023.

[8] S. Wu, T.X.Li, T.Yan, R.Z.Wang. Experimental investigation on a novel solid-gas thermochemical sorption heat transformer for energy upgrade with a large temperature lift. Energy Conversion and Management, 148(2017), 330-338.

[9] Johannessen T, Schmidt H, Svagin J, Oechsle J. Ammonia storage and delivery systems for automotive NOx aftertreatment. SAE Technical Paper 008-01-1027; 2008.

420 [10] Johannessen T. 3rd generation SCR system using solid ammonia storage and direct gas dosing: -
421 Expanding the SCR window for RDE. In: Directions in Engine Efficiency and Emissions Research (DEER)
422 Conference, Dearborn, Michigan, US, 2012.

423 [11] L. Jiang, X.L. Xie, L.W. Wang, R.Z. Wang, Y.D. Wang, A.P. Roskilly. Investigation on an innovative
424 sorption system to reduce nitrogen oxides of diesel engine by using carbon nanoparticle. Applied Thermal
425 Engineering, 134(2018) 29-38.

426 [12] Huashan Bao, Zhiwei Ma, Anthony Paul Roskilly. Chemisorption power generation driven by low grade
427 heat – Theoretical analysis and comparison with pumpless ORC. Applied Energy. 186(2017) 282-290.

428 [13] Neveu P, Castaing P. Solid-gas chemical heat pumps: Field of application and performance of the
429 internal heat of reaction recovery process. Heat Recovery Systems & CHP 1993;13: 233–51.

430 [14] OC Iloeje, AN Ndili, SO Enibe. Computer simulation of a $CaCl_2$ solid-adsorption solar refrigerator.
431 Energy 1995; 20:1141–1151.

432 [15] HJ Huang, GB Wu, J Yang, YC Dai, WK Yuan, HB Lu. Modeling of gas-solid chemisorption in
433 chemical heat pumps. Separation and Purification Technology 2004; 34:191–200.

434 [16] N Mazet, M Amouroux, B Spinner. Analysis and experimental study of the transformation of a non-
435 isothermal solid/gas reacting medium. Chemical Engineering Communications 1991; 99:155–174.

436 [17] E. Lepinasse, M. Marion, V. Goetz, Cooling storage with a resorption process. Application to a box
437 temperature control, Applied Thermal Engineering, 21 (2001) 1251-1263.

438 [18] L.Jiang, L.W. Wang, R.Z. Wang. Investigation on thermal conductive consolidated composite $CaCl_2$ for
439 adsorption refrigeration. International Journal of Thermal Sciences, 81(2014) 68-75.

[19] L.W. Wang, Z. Tamainot-Telto, S. J. Metcalf, R. E. Critoph, R. Z. Wang. Anisotropic thermal conductivity and permeability of compacted expanded natural graphite. Applied Thermal Engineering, 30 (2010) 1805-1811.

[20]Z. Q. Jin. Experiment on the thermal conductivity and permeability of physical and chemical compound adsorbents for sorption process. Heat and Mass Transfer. 2013 (49) 1117-1124.

[21] B. Tian, Z.Q. Jin, L.W. Wang, R.Z. Wang. Permeability and thermal conductivity of compact chemical and physical adsorbents with expanded natural graphite as host matrix. International Journal of Heat and Mass Transfer. 55(2012) 4453-4459.

[22] J. Gao, L.W. Wang, R.Z. Wang, Z.S. Zhou. Solution to the sorption hysteresis by novel compact composite multi-salt sorbents. Applied Thermal Engineering, 111(2017)580-585.

[23] H.W. Coleman, W.G. Steele Jr. Experimentation, validation and uncertainty analysis for Engineers. Wiley, 2009.

[24] Y. Zhong, R.E. Critoph, R.N. Thorpe, Z. Tamainot-Telto, Yu.I. Aristov. Isothermal sorption characteristics of the $BaCl_2$–NH_3 pair in a vermiculite host matrix. Applied Thermal Engineering, 27(2007) 2455-2462.

[25] I.A. Simonova, Yu.I. Aristov, Sorption properties of calcium nitrate dispersed in silica gel: the effect of pore size, Rus. J. Phys. Chem. 79 (8) (2005) 1307–1311.

[26] C. Wang, P. Zhang, R.Z. Wang. Investigation of soli-gas reaction heat transformer system with the consideration of multistep reactions. AIChE, 54(2008)2464-2478.

[27] J.H. Han, K.H. Lee, D.H. Kim, H. Kim. Transformation Analysis of Thermochemical Reactor Based on Thermophysical Properties of Graphite−$MnCl_2$ Complex. Industrial & Engineering Chemistry Research, 39 (2000) 4127-4139.